

## THE PHOTORESPONSE BEHAVIOR OF A MEH-PPV SENSITIZED TITANIUM DIOXIDE PHOTOELECTROCHEMICAL CELL

Assefa Sergawie\*, Teketel Yohannes and Theodros Solomon

Department of Chemistry, Addis Ababa University, P.O. Box 1176, Addis Ababa, Ethiopia

(Received September 26, 2006; revised October 26, 2006)

**ABSTRACT.** A solid-state photoelectrochemical cell based on polymer-sensitized nanocrystalline titanium dioxide (nc-TiO<sub>2</sub>) was constructed and studied for its photoresponse behavior. Poly[2-methoxy-5-(2-ethylhexyloxy)-1,4-phenylenevinylene] (MEH-PPV) and Poly[oxymethylene-oligo(oxyethylene)] (POMOE), complexed with I<sub>3</sub>/I redox couple were used as a polymer-sensitizer to TiO<sub>2</sub> and as a solid polymer electrolyte, respectively. The device produced a short-circuit current of 0.145 mA/cm<sup>2</sup>, and an open-circuit voltage of 410 mV under the irradiance of 100 mW/cm<sup>2</sup>. The power conversion efficiency and the fill factor were 0.03 % and 0.5, respectively. The monochromatic induced photon-to-current conversion efficiencies for backside (ITO/nc-TiO<sub>2</sub>/MEH-PPV) and for front side (ITO/PEDOT) illuminations were 1.8 % and 1.4 %, respectively.

**KEY WORDS:** Solid-state photoelectrochemical cell, Nanocrystalline titanium dioxide, MEH-PPV, POMOE, I<sub>3</sub>/I redox couple

### INTRODUCTION

Photoelectrochemical cells (PECs) utilize a dye to sensitize a wide band gap inorganic semiconductor. Dye-sensitized nc-TiO<sub>2</sub> PECs that use a ruthenium dye are considered as alternatives to conventional inorganic photovoltaic cells that convert solar energy to electricity [1]. The dye absorbs visible light and injects electrons to the conduction band of TiO<sub>2</sub> from which they are transferred to the external circuit. The I<sub>3</sub>/I redox couple present in the liquid electrolyte is used as a charge mediator. The power conversion efficiency of such cells reached 10.4 % [2, 3]. Despite their high power conversion efficiency, their commercial applications are limited due to problems like leakage of the electrolyte and the degradation of both the electrolyte [4] and the dye [5]. Various studies with different approaches have been carried out to alleviate the problems associated with liquid-state dye-sensitized nc-TiO<sub>2</sub> PECs. These include replacement of the liquid electrolyte by a polymer electrolyte [6] and by a hole-transporting material [7-10], replacement of the dye by a semiconducting polymer [11-13] and replacement of both the dye and the liquid electrolyte by a semiconducting polymer that plays the role of both a sensitizer and a hole-transporting medium [14-16].

The sensitizing effect of semiconducting polymers on nc-TiO<sub>2</sub> particles has been studied in different types of solar energy conversion devices. Photovoltaic cells based on composite films of nc-TiO<sub>2</sub> and MEH-PPV were studied [16, 17] where MEH-PPV was used both as a sensitizer to TiO<sub>2</sub> and as a hole-transporting medium. Such cells exhibited a monochromatic induced photon-to-current conversion efficiency of 6 % at the maximum absorption of the polymer [17]. Liquid-state photoelectrochemical cells using poly(3-thiophenemalononic acid)-sensitized TiO<sub>2</sub> electrodes were assembled with power conversion efficiency reaching 1.8 % [11]. In this work, we have designed a solid-state polymer-sensitized nc-TiO<sub>2</sub> PEC where MEH-PPV was used as a sensitizer to TiO<sub>2</sub> and the ion-conducting polymer; POMOE complexed with I<sub>3</sub>/I redox couple was used as a solid electrolyte. MEH-PPV was chosen because of its light absorption in the visible region, suitable energy positions of its highest occupied molecular orbital (HOMO) and

\*Corresponding author. E-mail: assefaserg@yahoo.com; Tel.: +251-91-1487557.

lowest unoccupied molecular orbital (LUMO) for charge transfer to nc-TiO<sub>2</sub> and to the electrolyte [18] and its low intrinsic trap density [19]. POMOE is known to have good ionic conductivity at room temperature [20]. As compared to liquid junction PECs, solid-state PECs have advantages like handling, portability and packaging while maintaining the advantages of the redox couple. Use of semiconducting polymers as sensitizers may be more advantageous than dye molecules with respect to the ease of large-scale production. Oxidized poly(3,4-ethylenedioxythiophene), PEDOT, electrochemically deposited on indium-doped tin oxide coated glass (ITO-glass) [21-23] was used as a counter electrode. PEDOT improves the charge transfer between the ITO and the I<sub>3</sub>/I<sup>-</sup> redox couple [24, 25]. The chemical structures of MEH-PPV and PEDOT are shown in Figure 1.

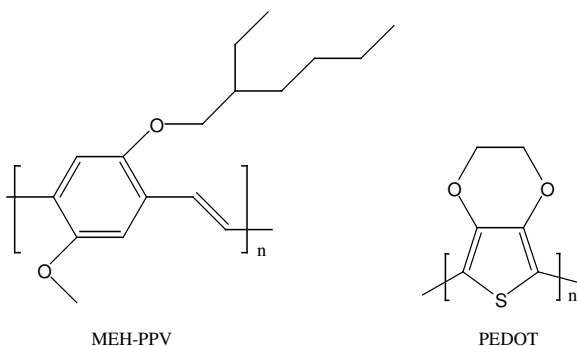


Figure 1. The chemical structure of poly[2-methoxy-5-(2-ethylhexyloxy)-1,4-phenylenevinylene], MEH-PPV and poly(3,4-ethylenedioxythiophene), PEDOT.

## EXPERIMENTAL

ITO-glass sheets (sheet resistance = 10 Ω/square), each of dimensions 1.5 cm x 2.5 cm were used as substrates. The ITO-glass substrates were cleaned successively with deionized water, acetone and isopropyl alcohol and dried in air. TiO<sub>2</sub> nanoparticles were formed by the hydrolysis of titanium isopropoxide according to literature [26, 27]. 0.5 mL of titanium isopropoxide (Aldrich, 99 %) was slowly added with vigorous stirring to a mixture of 2.5 mL of glacial acetic acid (Sigma Aldrich), 7.5 mL of isopropanol (Sigma Aldrich) and 2.5 mL of deionized water. The solution was stirred for three days to obtain a viscous solution. The colloidal TiO<sub>2</sub> solution was applied on the surface of the pre-cleaned ITO-glass and distributed with a glass rod sliding over an adhesive tape that covered the ITO-glass at the edges. The tape controlled the thickness of the TiO<sub>2</sub> film, which is in the range of few micrometers. A non-coated area (0.5 cm x 1.5 cm) was left for electrical contact. After drying in air, the TiO<sub>2</sub>-coated ITO-glass was sintered at 450 °C for 30 minutes in a furnace (Carbolite, ELF 11/14B model, England). 1.67 mg of MEH-PPV (Aldrich) was dissolved in 1 mL of 1,2-dichlorobenzene (Aldrich, 99 %). The MEH-PPV solution was drop-casted on the TiO<sub>2</sub>-coated ITO-glass. It was then dried in air at room temperature. The slow evaporation of the solvent at room temperature resulted in the formation of a uniform film of MEH-PPV. After heating the composite film at 30 °C for six hours, the polymer electrolyte (POMOE) complexed with I<sub>3</sub>/I<sup>-</sup> redox couple was drop-casted on the top of the nc-TiO<sub>2</sub>/MEH-PPV film from methanol solution and dried in air. The I<sub>3</sub>/I<sup>-</sup> was prepared by dissolving 47.4 mg KI and 7.2 mg I<sub>2</sub> in 25 mL of methanol separately. Similarly, 304.2 mg of POMOE was dissolved in 25 mL of methanol. Finally, equal volumes of each solution were

mixed to produce the polymer electrolyte complexed with I<sub>3</sub><sup>-</sup>/I<sup>-</sup>. The mole ratio of oxygen to potassium as calculated by taking into account both the oxymethylene and oxyethylene oxygen atoms was 25 and the mole ratio of KI to I<sub>2</sub> was 10:1. PEDOT was electrochemically polymerized on ITO-glass from a solution of 0.1 M 3,4-ethylenedioxythiophene, EDOT (Bayer), in acetonitrile that contains 0.1 M LiClO<sub>4</sub>. The polymerization was carried out potentiostatically at 1.8 V (vs. Ag/AgCl quasi-reference electrode) for 4 seconds. The film formed was semitransparent. Contacting the photoactive electrode with the counter electrode (oxidized PEDOT) completed the cell. Contact between the electrodes was ensured by the application of pressure using a spring attached to a sample holder. The PEC was then mounted in a sample holder inside a metal box having a 1 cm x 1 cm light entrance window, which determined the illumination area.

A 250 W tungsten-halogen lamp regulated by an Oriel power supply (Model 66182) was used to illuminate the PEC. For spectral studies, a grating monochromator (Model 77250) was used to select a wavelength manually between 300 nm and 800 nm at an interval of 10 nm. The steady-state current was recorded after illuminating the device for 60 seconds at each selected wavelength. All spectra were corrected for the spectral response of the lamp and the monochromator by normalization to the response of a calibrated silicon photodiode (Hamamatsu, model S-1336-8BK). The white light intensity was measured in the position of the sample cell with a Conrad electronic luxmeter (Model LX-101). For intensity dependence measurements a series of neutral density filters were placed between the light source and the sample holder to vary the light intensity incident on the sample. The photoelectrochemical properties were studied using CHI600A Electrochemical Analyzer. Optical absorption measurements were carried out using a Perkin-Elmer Lambda 19 UV/VIS/NIR spectrometer.

## RESULTS AND DISCUSSION

### *Current-voltage characteristics*

The current–voltage characteristics of the ITO/nc-TiO<sub>2</sub>/MEH-PPV/(I<sub>3</sub><sup>-</sup>/I<sup>-</sup>)/PEDOT/ITO solid-state PEC in the dark and under white light illumination from the backside at light intensity of 100 mW/cm<sup>2</sup> is shown in Figure 2. The device did not give a significant dark current for a certain range of applied voltages. The illuminated cell delivered an anodic short-circuit current (I<sub>SC</sub>) of 0.145 mA/cm<sup>2</sup> and an open-circuit voltage (V<sub>OC</sub>) of 410 mV. The fill factor (FF) and the power conversion efficiency (η) of the device were 0.5 and 0.03 %, respectively. The fill factor and the power conversion efficiency (%) were calculated using Equation (1) and Equation (2), respectively, where the product (I x V)<sub>MAX</sub> is the maximum power delivered by the device and P<sub>in</sub> is the power of the incident light.

$$FF = \frac{(IV)_{MAX}}{I_{SC} V_{OC}} \quad (1)$$

$$\eta(\%) = \frac{(IV)_{MAX}}{P_{in}} \times 100 \quad (2)$$

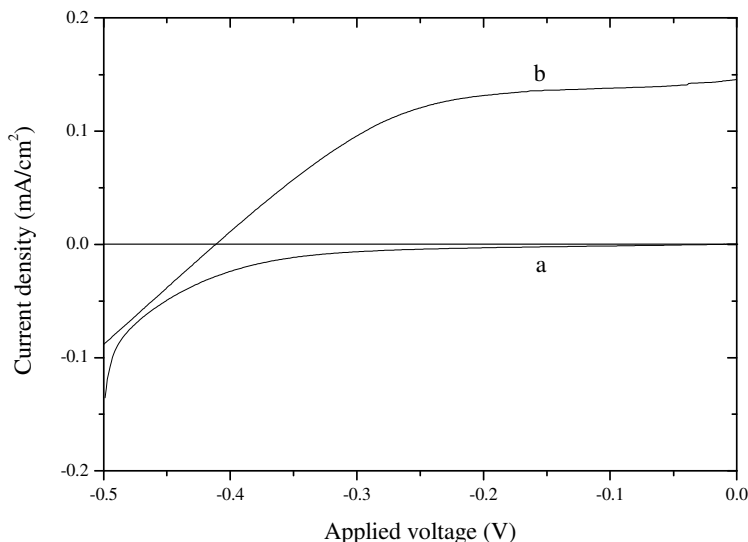


Figure 2. Current density *versus* voltage characteristics of the nc-TiO<sub>2</sub>/MEH-PPV based solid-state PEC (a) in the dark and (b) under white light illumination from the backside at light intensity of 100 mW/cm<sup>2</sup>.

#### *Time dependence of the short-circuit current density and the open-circuit voltage*

The changes in  $I_{SC}$  and  $V_{OC}$  with and without illumination were measured as a function of time. These measurements were used to observe the transient response of the cell and its stability towards light illumination. The illumination was made from the backside with white light of intensity 100 mW/cm<sup>2</sup> and it was switched on and off periodically by blocking the light path. Upon illumination a transient short-circuit current was immediately generated, probably due to rapid modifications in the electrical properties of the semiconducting polymer [28]. The short-circuit current then dropped and came to a steady-state value of 0.145 mA/cm<sup>2</sup> (Figure 3). An increase in the photocurrent was observed during continuous illumination. When the illumination was switched off, the current immediately dropped to zero. An open-circuit photovoltage was also immediately generated with a value of 410 mV and dropped to zero sharply when the illumination was switched off indicating the absence of electron trapping sites on the composite film (Figure 4). Such behaviors of  $I_{SC}$  and  $V_{OC}$  have been observed in a similar photoelectrochemical system without TiO<sub>2</sub> [29].

#### *Spectral response*

The photocurrent collected at different wavelengths of the incident light, relative to the number of photons incident on the surface at that wavelength, determines the spectral response of a PEC. The ability of a solar cell to generate photocurrent at a given wavelength of the incident light is measured by the monochromatic incident photon-to-current conversion efficiency (IPCE), defined as the number of electrons generated per number of incident photons. It can be obtained from the photocurrent at each wavelength using Equation (3) where  $I_{SC}$  is the short circuit current density ( $\mu\text{A}/\text{cm}^2$ ),  $\lambda$  is the excitation wavelength (nm) and  $I_{in}$  is the incident photon intensity ( $\text{W}/\text{m}^2$ ).

$$IPCE\% = \frac{1240I_{sc}}{\lambda I_{in}} \quad (3)$$

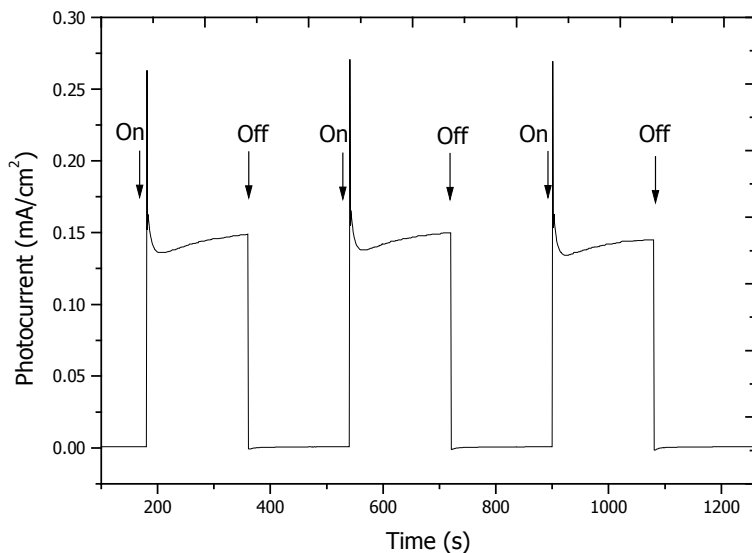


Figure 3. Short-circuit photocurrent changes induced by switching illumination on and off from the backside of the nc-TiO<sub>2</sub>/MEH-PPV based solid-state PEC with incident light intensity of 100 mW/cm<sup>2</sup>.

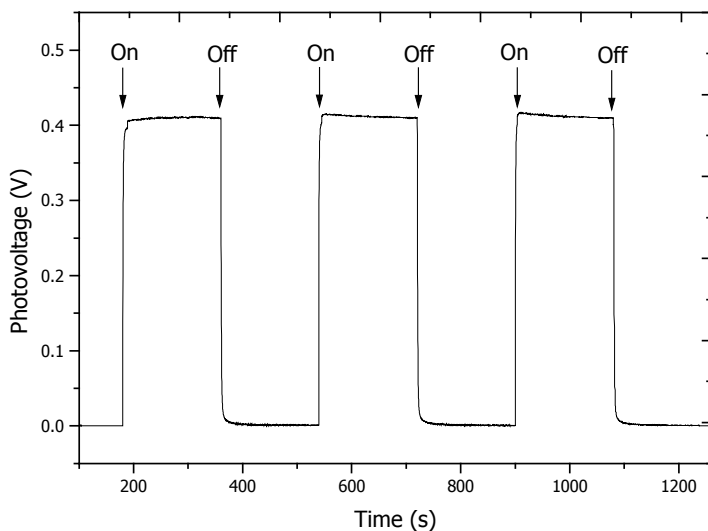


Figure 4. Open-circuit voltage response of the nc-TiO<sub>2</sub>/MEH-PPV based solid-state PEC to switching illumination on and off from the backside with incident light intensity of 100 mW/cm<sup>2</sup>.

Figure 5 shows the UV-Visible absorption spectrum of MEH-PPV and the IPCE spectra for the backside and for the front side illumination of a nc-TiO<sub>2</sub>/MEH-PPV based solid-state PEC under short-circuit condition. The Figure shows that the IPCE spectra for backside and front side illuminations closely match the absorption spectrum of MEH-PPV indicating that the photoelectrochemical conversion is achieved through the photosensitization of TiO<sub>2</sub> by MEH-PPV. The IPCE % obtained for the backside and for the front side illuminations at the maximum absorption of MEH-PPV (500 nm) were 1.8 % and 1.4 %, respectively. The higher IPCE for the backside illumination indicates that excitons are generated near the nc-TiO<sub>2</sub>/MEH-PPV interface where exciton dissociation takes place [30]. The lowering of the IPCE for front side illumination could be due to electron recombination processes during the transport of electron-hole pair (exciton) from the outer part of the film to the nc-TiO<sub>2</sub>/MEH-PPV interface [31].

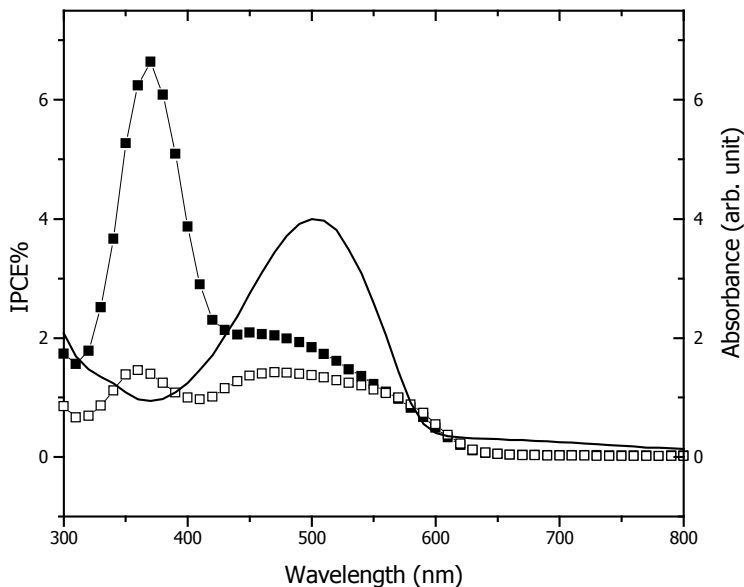


Figure 5. Optical absorption spectrum of MEH-PPV film (solid line) and the photocurrent action spectra of nc-TiO<sub>2</sub>/MEH-PPV based PEC under illumination from the backside (solid squares) and front side (open squares).

The IPCE peak observed at shorter wavelengths (around 380 nm) is due to light absorption by the nc-TiO<sub>2</sub>. The value is relatively high (especially during backside illumination where exciton dissociation is favored) because of the low light intensities in the short wavelength regions (Figure 6). Figure 6 (from which the IPCE spectra of Figure 5 are obtained) shows the incident light intensity distribution at the sample position and the short-circuit current density which were measured at different wavelengths while illuminating a calibrated silicon photodiode and the nc-TiO<sub>2</sub>/MEH-PPV based solid-state PEC, respectively. From Figure 6, it can be observed that much of the current during white light illumination comes from the sensitizing effect of MEH-PPV.

Figure 7 illustrates the schematic of operation of the nc-TiO<sub>2</sub>/MEH-PPV based solid-state PEC. The energy levels of the LUMO and the HOMO of MEH-PPV are at -2.9 eV and -5.1 eV *vs.* vacuum, respectively [18]. The quasi-Fermi energy level of nc-TiO<sub>2</sub> under illumination is -4.2 eV *vs.* vacuum [32]. Thus photogenerated free electrons can be

transferred from the LUMO of MEH-PPV to the low-lying conduction band of TiO<sub>2</sub>. In the mean time photogenerated holes can be transferred from the HOMO of MEH-PPV to the electrolyte where they oxidize  $\Gamma^-$  to  $I_3^-$  ( $E_{\text{redox}}(I_3^-/\Gamma^-) = -4.9$  eV vs. vacuum [3]).  $\Gamma^-$  is regenerated when the  $I_3^-$  is reduced at the counter electrode.

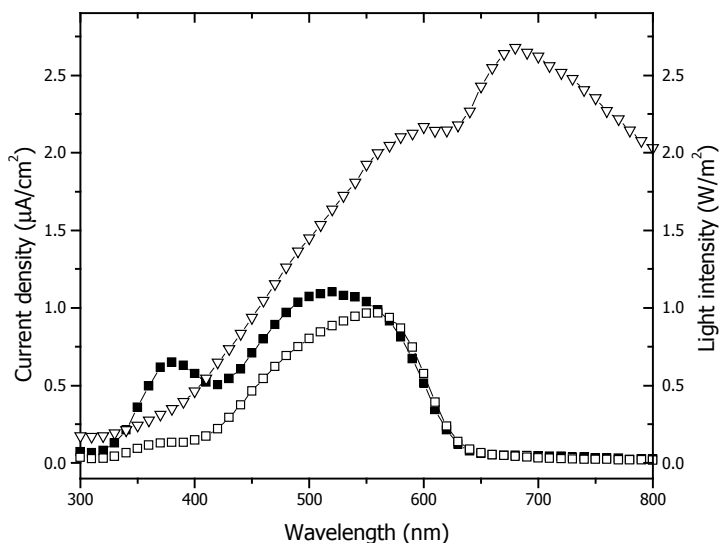


Figure 6. Incident light intensity distribution (open triangles) and short-circuit photocurrent density spectra of the nc-TiO<sub>2</sub>/MEH-PPV based solid-state PEC under illumination from the backside (solid squares) and front side (open squares).

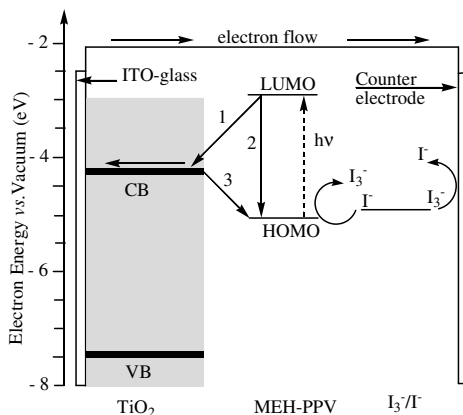


Figure 7. Schematic of operation of the nc-TiO<sub>2</sub>/MEH-PPV based solid-state PEC. The photoanode, made of MEH-PPV-sensitized nc-TiO<sub>2</sub>, receives electrons from the photoexcited MEH-PPV (path 1). The oxidized MEH-PPV is returned to its neutral state by receiving electrons from the reduced form ( $\Gamma^-$ ) of the redox couple ( $I_3^-/\Gamma^-$ ). The  $\Gamma^-$  is regenerated by the reduction of  $I_3^-$  at the counter electrode by the electrons circulated through the external circuit. Path 2 and path 3 refer to charge recombination processes.

### Dependence of $I_{sc}$ and $V_{oc}$ on incident light intensity

The  $I$ - $V$  characteristics of an illuminated semiconductor electrode in a PEC can be obtained using the diode equation (Equation (4)) where  $I$  is the net current density,  $I_0$  is the exchange current density,  $I_{ph}$  is the photogenerated minority carrier current density,  $q$  is the electronic charge,  $k$  is the Boltzmann constant,  $T$  is the absolute temperature and  $V$  is the applied voltage.

$$I = I_{ph} - I_0 \left[ \exp\left(\frac{qV}{nkT}\right) \right] - 1 \quad (4)$$

$V_{OC}$  can be obtained by letting the net current be zero. When  $I_{ph} > I_0$ , which is generally the case, Equation (4) reduces to Equation (5).

$$V_{OC} = \frac{nkT}{q} \ln \left[ \frac{I_{ph}}{I_0} \right] \quad (5)$$

From Equation (5),  $V_{OC}$  increases logarithmically with the light intensity, because  $I_{ph}$  is linearly proportional to the absorbed photon flux. Similarly,  $I_{SC}$  can be computed by letting  $V = 0$  into Equation (4) that reduces to Equation (6).

$$I_{SC} = I_{ph} \quad (6)$$

Since  $I_{ph}$  depends linearly on light intensity, the short-circuit current increases linearly with increasing light intensity and is proportional to  $P_{in}^\alpha$  [33] where  $\alpha$  is the power factor and  $P_{in}$  is the incident light intensity. The plots of  $\log I_{SC}$  and  $V_{OC}$  versus  $\log P_{in}$  for nc-TiO<sub>2</sub>/MEH-PPV based solid-state PEC are depicted in Figures 8 and 9, respectively. The plot of  $\log I_{SC}$  versus  $\log P_{in}$  yielded a straight line with  $\alpha = 0.9$ . An  $\alpha$  value less than 1 indicates the presence of some exciton recombination due to surface states that act as recombination centers [33, 34].

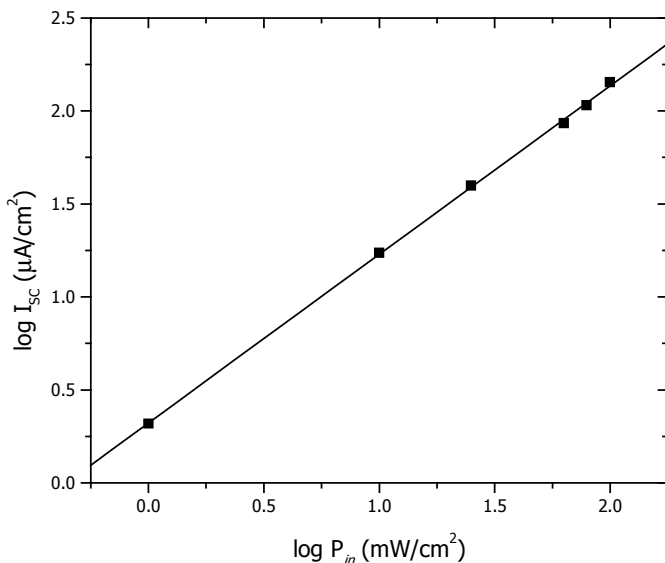


Figure 8. Dependence of short-circuit photocurrent on incident light intensity for illumination through the backside of the nc-TiO<sub>2</sub>/MEH-PPV based solid-state PEC.

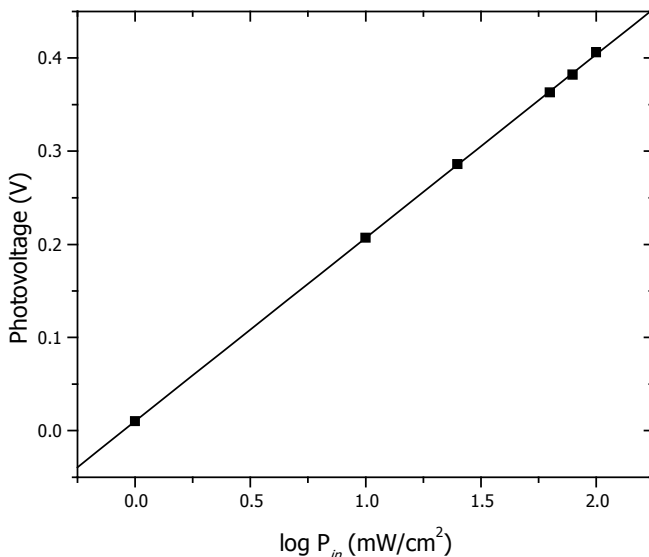


Figure 9. Dependence of photovoltage on incident light intensity for illumination through the backside of the nc-TiO<sub>2</sub>/MEH-PPV based solid-state PEC.

## CONCLUSIONS

A solid-state PEC based on MEH-PPV-sensitized TiO<sub>2</sub> was constructed and studied for its photoresponse behavior. The solid polymer electrolyte used in the device was POMOE that was complexed with I<sub>3</sub><sup>-</sup>/I<sup>-</sup> and the counter electrode was oxidized PEDOT on ITO-glass. A short-circuit current of 0.145 mA/cm<sup>2</sup>, an open-circuit voltage of 410 mV, a power conversion efficiency of 0.03 % and a fill factor of 0.5 were obtained when the device was illuminated with light of intensity 100 mW/cm<sup>2</sup>. The IPCE % obtained for the backside and for the front side illuminations at the maximum absorption of MEH-PPV (500 nm) were 1.8 % and 1.4 %, respectively. Exciton recombination may be a limiting factor for the photocurrent generation as observed from the study of incident light intensity dependence of short-circuit current. Though the performance of the device is low when compared with solid-state dye-sensitized and liquid-state polymer-sensitized nc-TiO<sub>2</sub> photoelectrochemical cells, the results are still encouraging when considering the advantages of conducting polymers and polymer electrolytes over dyes and liquid electrolytes, respectively. Increasing the interpenetration of the sensitizing polymer and the polymer electrolyte through the pores of the nc-TiO<sub>2</sub> particles, use of a sensitizing polymer that could be adsorbed better on to the nc-TiO<sub>2</sub> particles and use of a polymer electrolyte with better conductivity can increase the power conversion efficiencies of polymer-sensitized solid-state photoelectrochemical cells.

## ACKNOWLEDGEMENTS

The authors thank the Ethiopian Science and Technology Agency, the Third World Academy of Sciences, Trieste, Italy and SIDA/SAREC for financial support. The authors gratefully thank Prof. N.S. Sariciftci, Linz Institute for Organic Solar Cells, for providing chemicals.

## REFERENCES

1. O'Regan, B.; Grätzel, M. *Nature* **1991**, 353, 737.
2. Nazeeruddin, M.K.; Kay, A.; Rodicio, I.; Humphry-Baker, R.; Müller, E.; Liska, P.; Vlachopoulos, N.; Grätzel, M. *J. Am. Chem. Soc.* **1993**, 115, 6382.
3. Hagfeldt, A.; Grätzel, M. *Acc. Chem. Res.* **2000**, 33, 269.
4. Hinsch, A.; Kroon, J.M.; Kern, R.; Uhlendorf, I.; Holzbock, J.; Meyer, A.; Ferber, J.A. *Prog. Photovolt: Res. Appl.* **2001**, 9, 425.
5. Grünwald, R.; Tributsch, H. *J. Phys. Chem. B* **1997**, 101, 2564.
6. Nogueira, A.F.; Durrant, J.R.; De Paoli, M.A. *Adv. Mater.* **2001**, 13, 826.
7. O'Regan, B.; Schwartz, D.T. *J. Appl. Phys.* **1996**, 80, 4749.
8. Bach, U.; Lupo, D.; Comte, P.; Moser, J.E.; Weissörtel, F.; Salbeck, J.; Spreitzer, H.; Grätzel, M. *Nature* **1998**, 395, 583.
9. Gebeyehu, D.; Brabec, C.J.; Sariciftci, N.S.; Vangeneugden, D.; Kiebooms, R.; Vanderzande, D.; Kienberger, F.; Schindler, H. *Synth. Met.* **2002**, 125, 2797.
10. Gebeyehu, D.; Brabec, C.J.; Padinger, F.; Fromherz, T.; Spiekermann, S.; Vlachopoulos, N.; Kienberger, F.; Schindler, H.; Sariciftci, N.S. *Synth. Met.* **2001**, 121, 1549.
11. Senadeera, G.K.R.; Kitamura, T.; Wada, Y.; Yanagida, S. *Sol. Energy Mater. Sol. Cells* **2005**, 88, 315.
12. Hao, Y.; Yang, M.; Yu, C.; Cai, S.; Liu, M.; Fan, L.; Li, Y. *Sol. Energy Mater. Sol. Cells* **1998**, 56, 75.
13. Van Hal, P.A.; Wienk, M.M.; Kroon, J.M.; Janssen, R.A.J. *J. Mater. Chem.* **2003**, 13, 1054.
14. Van Hal, P.A.; Wienk, M.M.; Kroon, J.M.; Verhees, W.J.H.; Slooff, L.H.; van Gennip, W.J.H.; Jonkheijm, P.; Janssen, R.A.J. *Adv. Mater.* **2003**, 15, 118.
15. Gebeyehu, D.; Brabec, C.J.; Sariciftci, N.S. *Thin Solid Films* **2002**, 271, 403.
16. Savenije, T.J.; Warman, J.M.; Goossens, A. *Chem. Phys. Lett.* **1998**, 287, 148.
17. Breeze, A.J.; Schlesinger, Z.; Brock, P.J.; Carter, S.A. *Phys. Rev. B* **2001**, 64, 125205.
18. Li, Y.; Cao, Y.; Gao, J.; Wang, D.; Yu, G.; Heeger, A.J. *Synth. Met.* **1999**, 99, 243.
19. Bozano, L.; Carter, S.A.; Scott, J.C.; Malliaras, G.G.; Brock, P.J. *Appl. Phys. Lett.* **1999**, 74, 1132.
20. Nagae, S.; Nekoomanesh, H.M.; Booth, C.; Owen, J.R. *Solid State Ionics* **1992**, 1118, 53.
21. Pei, Q.; Ahlskog, M.; Inganäs, O. *Polymer* **1994**, 35, 1347.
22. Chen, X.; Xing, K.-Z.; Inganäs, O. *Chem. Mater.* **1996**, 8, 2439.
23. Randriamahazaka, H.; Noël, C.; Chevrot, C. *J. Electroanal. Chem.* **1999**, 472, 103.
24. Granström, M.; Petritsch, K.; Arias, A.C.; Lux, A.; Andersson, M.R.; Friend, R.H. *Nature* **1998**, 395, 257.
25. Yohannes, T.; Inganäs, O. *Sol. Energy Mater. Sol. Cells* **1998**, 51, 193.
26. Grant, C.D.; Schwartyberg, A.M.; Smestad, G.P.; Kowalik, J.; Tolbert, L.M.; Zhang, J.Z. *J. Electroanal. Chem.* **2002**, 522, 40.
27. Tennakone, K.; Kumara, G.R.R.A.; Kottegoda, I.R.M.; Wijayantha, K.G.U.; Perera, V.P.S. *J. Phys. D: Appl. Phys.* **1998**, 31, 1492.
28. Genies, E.M.; Lapkowski, M. *Synth. Met.* **1988**, 24, 69.
29. Yohannes, T.; Inganäs, O. *J. Electrochem. Soc.* **1996**, 143, 2310.
30. Arango, A.C.; Johnson, L.; Horhold, H.; Schlesinger, Z.; Carter, S.A. *Adv. Mater.* **2000**, 12, 1689.
31. Lindström, H.; Hagfeldt, A.; Rensmo, H.; Solbrand, A.; Södergren, S.; Lindquist, S.E. *SPIE* **1995**, 2531, 176.
32. Hagfeldt, A.; Grätzel, M. *Chem. Rev.* **1995**, 95, 49.
33. Meier, H. *Organic Semiconductors*, Verlag Chemi: Berlin; **1974**; p 318.
34. Loufty, R.O.; Sharp, J.H.; Hsiao, C.K.; Ho, R. *J. Appl. Phys.* **1981**, 52, 5218.